

## Development of biodegradable polymeric nanoparticles for encapsulation, delivery, and improved antifungal performance of natamycin

Clotilde Bouaoud,<sup>1,2</sup> Sala Xu,<sup>1</sup> Eduardo Mendes,<sup>2</sup> Jérôme G. J. L. Lebouille,<sup>3</sup>  
Henriette E. A. De Braal,<sup>1</sup> Gabriel M. H. Meesters<sup>1,2</sup>

<sup>1</sup>DSM Food Specialties, DSM Biotechnology Center, Alexander Fleminglaan 1 2613 AX Delft, The Netherlands

<sup>2</sup>Department of Chemical Engineering, Delft University of Technology, Julianalaan 136, Delft, BL, 2628, The Netherlands

<sup>3</sup>DSM Biomedical, Chemelot, Urmonderbaan 22, Geleen, 6167RD, The Netherlands

Correspondence to: C. Bouaoud (E-mail: cbouaoud@gmail.com)

**ABSTRACT:** The aim of this study was to evaluate biodegradable poly(lactide-co-glycolide) nanoparticles as potential nano-delivery systems for the food antifungal compound natamycin. Natamycin-loaded nanoparticles were prepared at various ratios polymer/antifungal by the nanoprecipitation technique, resulting in nano-size particles (80–120 nm) with a narrow distribution and a spherical morphology. Complexation of natamycin with PLGA and active participation to the nanoparticle formation were evidenced by a mean diameter reduction of 10–30 nm, although encapsulation levels remained low due to the zwitterionic and partially hydrophilic nature of natamycin. Physical state analyses highlighted the presence of natamycin in an amorphous or molecularly dispersed state within the polymeric matrix. This translates into high availability of free antifungal molecules reflected in burst release and fast *in vitro* release kinetics rates as well as enhanced antifungal performance against the model food yeast *Saccharomyces cerevisiae*, offering a potential benefit for antifungal protection compared with the commercially available natamycin products. © 2016 Wiley Periodicals, Inc. *J. Appl. Polym. Sci.* **2016**, *133*, 43736.

**KEYWORDS:** applications; biodegradable; characterization; nanoparticles; nanowires and nanocrystals; polyesters; properties

Received 1 January 2016; accepted 4 April 2016

DOI: 10.1002/app.43736

### INTRODUCTION

Natamycin<sup>1–3</sup> (Figure 1), also known as pimaricin, is one of the most popular biopreservative compounds currently involved in food protection.<sup>4,5</sup> Produced by fermentation of *Streptomyces natalensis*, a Gram-positive bacteria strain originated from the province of Natal in South Africa, natamycin is a natural polyene macrolide antimycotic that possesses a broad activity spectrum against yeast and molds, efficacy at low doses (1–3 ppm against most known food microbes) and activity over a wide range of pH with no reported resistance since its discovery 50 years ago. The mechanism of antifungal action of this biopreservative has been recently explained by the diffusion and binding of natamycin molecules to the ergosterol present in biological membranes.<sup>6</sup> When incorporated or applied on food products, this compound has the advantage over other antifungals to not affect the food quality (taste, color, odor) and to have a long history of safe use. The main applications of this biopreservative in the past decades focused on the long-term protection of food surfaces of cheese and fermented meat like sausages, by applying

coatings containing the preservative as crystalline particles that dissolve slowly and liberate free molecules that are able to participate to the antifungal activity. More recently, applications by direct incorporation of natamycin crystals in food products such as yoghurts, beverages, wines or baked goods have emerged in some countries and have been approved by the Food and Drug Administration (FDA).

Despite its worldwide use, developing natamycin formulations ensuring both efficient and targeted antifungal activity remains demanding. Current commercial formulations of natamycin are indeed based exclusively on crystalline particles, which offer limited selectivity and tunability of antifungal action or release profiles, narrowing the efficiency and the range of possible food applications for this biopreservative. More importantly, natamycin present a low aqueous solubility (20–50 ppm),<sup>1</sup> explained by its tendency to crystallize and its complex chemical structure combining a macrocycle—with opposite sides presenting different levels of polarity and rigidity—and a zwitterionic nature due to the presence of a carboxylic acid and an amino group

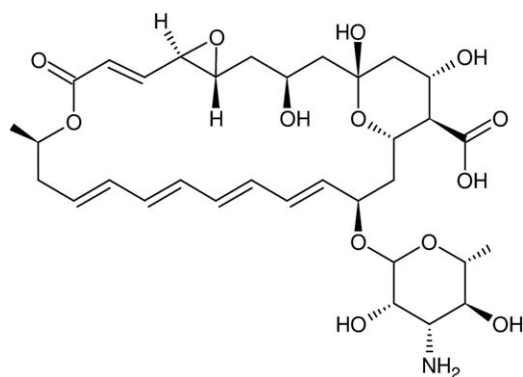


Figure 1. Molecular structure of natamycin.

[( $pK_a$  4–4.5,  $pK_b$  8.6, isoelectric point around pH 6.5)]. When applied as crystals in food products, this poor solubility leads to slow dissolution, limited amount of free molecules available for the antifungal activity as well as slow diffusion rate of the preservative to the sites of antifungal action. In the specific case of food coatings, this often results in heterogeneous surface protection and challenges to maintain locally a concentration of preservative superior to the minimum inhibitory concentration required towards micro-organisms. While increasing the initial amount of natamycin crystals incorporated or repeating the antifungal treatment at several occasions could be methods to implement to ensure food protection on the long term, these options remain strongly restricted by food regulations in terms of acceptable preservative levels, by growing demand of the consumers for reduced treatments and by possible formulation incompatibilities during application (e.g., undesired visual appearance of particles in coatings or settlement in suspensions).

Nano-encapsulation systems have for several years attracted the attention of the food industry and could bring a more complete answer to the issues encountered for natamycin. Nano-encapsulation systems could indeed provide higher availability and improved antifungal efficiency of natamycin.<sup>7,8</sup> Bhatta *et al.* already described for example the inclusion of natamycin in chitosan/lecithins mucoadhesive nanoparticles and demonstrated a clear benefit of the nanoformulation for prolonged ocular delivery.<sup>9</sup> Similar increase of performance, improvement of solubility and controlled release for ocular delivery were observed by incorporating the preservative in biodegradable core-shell micelles obtained by self-assembly of linear amphiphilic poly (*D,L*-lactide)-dextran block copolymer as reported by Phan *et al.*<sup>10</sup> More recently, our group also demonstrated the benefits of encapsulation of natamycin within soybean nano-liposomes for an enhanced antifungal activity and development of tunable release profiles.<sup>11</sup> In addition to these antimicrobial efficiency benefits, the well-known specific physicochemical properties of nanoparticles could also be useful compared with crystals for an easier incorporation into food applications, allowing for instance a superior and more homogeneous surface coverage and protection in food coatings or preventing settlement while used in suspensions.

To our knowledge, biodegradable polymeric nanospheres—that is, spherical matrix-type colloidal particles whose entire mass is

solid—have not been reported yet as nano-delivery systems for natamycin. Biodegradable polymeric nanospheres are characterized by a size usually ranging between several tenths of nanometers to a few hundreds, with the active ingredient to encapsulate and deliver being dissolved or entrapped within the matrix and/or adsorbed at the surface via interactions with the polymer forming the nanospheres.<sup>12,13</sup> Preformed polyesters like poly (lactic-co-glycolic acid) (PLGA) are part of the polymers commonly used, due to their approval by the FDA, their good biocompatibility and the wide range of degradation behaviors thus tunable release rates that they offer. Biodegradable polymeric nanospheres have proven to be valuable for the encapsulation and improvement of antimicrobial properties of various antibacterial and antifungal agents, among which other polyene macrolides from the same chemical family than natamycin such as amphotericin B and nystatin.<sup>14–19</sup> Biodegradable polymeric nanospheres have also been extensively described as interesting nano-carriers for the encapsulation of both hydrophilic and lipophilic molecules and are expected to allow encapsulation natamycin despite its complex and zwitterionic nature.

The aim of the present study was to assess the benefits related to the use of this type of nano-carriers for the encapsulation, delivery and antifungal performance of natamycin, compared with the currently commercial formulation consisting of a simple suspension of crystalline natamycin particles in water. Natamycin-loaded PLGA nanoparticles were prepared by nanoprecipitation.<sup>20</sup> Physicochemical characteristics of the nanoparticles were assessed by particle size analysis, zeta-potential determination, encapsulation, and loading efficiencies determination, TEM, DSC, and X-ray diffraction. The release kinetics of natamycin from PLGA nanoparticles were also investigated as well as antifungal performance against the model yeast *Saccharomyces cerevisiae* using agar disk diffusion assay.

This study evidenced that natamycin-loaded PLGA nanoparticles prepared by nanoprecipitation—despite limited entrapment levels due to the chemical properties of natamycin—could offer a beneficial fast release profile and enhanced antifungal activity compared with commercial crystalline natamycin formulations and represents an advantage for the treatment of food products for which high levels of antifungal protection are required at early stages of their preparation.

## EXPERIMENTAL

### Materials

Natamycin (90.6% purity, trihydrate crystalline form) was kindly supplied by DSM Food Specialties (Delft, The Netherlands). PLGA (Resomer<sup>®</sup> RG752H, 75:25 lactide:glycolide, molecular weight 4–15 kDa) was purchased from Sigma-Aldrich (St Louis, MO). Methanol EMSURE<sup>®</sup> ACS and anhydrous acetone Seccosolv<sup>®</sup> were purchased from Merck (Darmstadt, Germany) and used for the preparation of the nanoparticles. Potassium dihydrogen phosphate, methanol and acetonitrile Lichrosolv<sup>®</sup> were obtained from Merck and used for HPLC analyses. High quality water purified in a Milli-Q system was used in all experiments.

### Preparation of Polymeric Nanoparticles

PLGA nanoparticles were prepared by the nanoprecipitation technique. Briefly, PLGA was dissolved at room temperature in anhydrous acetone (15 or 37.5 mg/mL) while natamycin was dissolved in methanol (0.5–2.5 mg/mL). Both solutions were mixed at a ratio acetone/methanol 2:1 v/v. This organic phase was injected by one-shot addition using an Eppendorf pipette at a ratio of 4% v/v into MilliQ water under moderate magnetic stirring (500 rpm). The resulting nanosuspension was kept under slow stirring (200 rpm) overnight for evaporation of the organic solvent. Unloaded PLGA nanoparticles were prepared by the same method, omitting the incorporation of natamycin in methanol.

Loaded and unloaded PLGA nanosuspensions were used as such or lyophilized if required for physicochemical analyses. Freeze-drying was performed with 2 mL of nanosuspension, in the absence of cryoprotectant, using an industrial Advantage 2.0 Bench Top freeze-dryer Model XL (VirTis Advantage, SP Scientific, New York). The freeze-drying cycle consisted in a first ramp freezing step (25 to  $-60^{\circ}\text{C}$  at  $1.5^{\circ}\text{C}/\text{min}$ , 180 min hold at  $-60^{\circ}\text{C}$ ), followed by a primary drying step ( $-50^{\circ}\text{C}$ , 60  $\mu\text{bar}$ , 2000 min) and a secondary drying step ( $20^{\circ}\text{C}$ , 50  $\mu\text{bar}$ , 480 min). Lyophilized nanopowders were stored in sealed vials at  $4^{\circ}\text{C}$  until further use.

### Physicochemical Characterization of Nanoparticles

**Particle Size and Zeta-Potential.** The mean particle diameter and polydispersity index (Pdl) of the nanoparticles were determined by Dynamic Light Scattering (DLS) (Zetasizer Nano ZS, Malvern Instruments Ltd., UK). Three consecutive measurements were performed on each nanosuspension at  $25^{\circ}\text{C}$  at a scattering angle of  $173^{\circ}$ , after an equilibration time of 180 seconds. The electrical charge of the nanoparticles (zeta-potential  $\zeta$ ), was assessed on undiluted nano-suspensions with the same equipment. Zeta-potentials were obtained by three consecutive measurements at  $25^{\circ}\text{C}$  after an equilibration time of 180 sec-

onds. All measurements were performed in triplicate and results are presented as mean  $\pm$  standard deviation (SD).

**Morphology.** The morphology of PLGA nanoparticles was investigated using transmission electron microscopy (TEM) (Tecnai G<sup>2</sup>, FEI, Hillsboro) with an acceleration voltage of 200 kV. Prior to examination, samples were submitted to negative staining by mixing 20  $\mu\text{L}$  of solvent-free nanosuspension with 20  $\mu\text{L}$  of a 2% w/v neutralized phosphotungstic acid solution. About 10  $\mu\text{L}$  of the mixture were placed on a Formvar-coated grid (Copper with Formvar 0.5%, 200 mesh) and allowed to adsorb for 90 s. After blotting off excess solution, the grid was left to dry at room temperature overnight before analysis.

**Encapsulation (EE) and Loading Efficiencies (LE).** Content of natamycin in the nanoparticles was determined by reverse-phase high-performance liquid chromatography (HPLC). A high pressure liquid chromatograph Ultimate 3000 Dionex equipped with a variable wavelength detector was used. Separation was achieved by injecting 20  $\mu\text{L}$  of sample on a reverse phase column Licospher<sup>®</sup> RP18 (Merck, 125 nm  $\times$  4 mm, pore size 100  $\text{\AA}$ ) with a mobile phase consisting of 35:65 v/v acetonitrile: potassium dihydrogenphosphate buffer (pH 3.05) at a flow rate of 1.0 mL/min. Natamycin was detected by UV at a wavelength of 303 nm and quantified using a calibration curve designed over the range 0.05–50 ppm ( $R^2 = 0.9996$ ). All HPLC samples were analyzed in triplicates. Total amount of natamycin was obtained by dilution of an aliquot of the nano-suspension in acetonitrile/methanol 50/50 v/v. Amount of free natamycin in solution was obtained by subjecting the nano-suspensions to ultracentrifugation (Beckman Coulter L8-70M, rotor 50, 50,000 rpm, 1 h,  $10^{\circ}\text{C}$ ). An aliquot of the supernatant was withdrawn and diluted with the mixture acetonitrile/methanol. EE and LE were calculated according to eqs. (1) and (2). Determination of EE and LE was performed on three samples for each composition. Results are presented as mean  $\pm$  standard deviation.

$$\text{EE (\%)} = \frac{\text{Total amount of natamycin} - \text{Amount of natamycin in the supernatant}}{\text{Total amount of natamycin}} \times 100 \quad (1)$$

$$\text{LE (\%)} = \frac{\text{Total amount of natamycin} - \text{Amount of natamycin in the supernatant}}{\text{Amount of nanoparticles}} \times 100 \quad (2)$$

**Differential Scanning Calorimetry (DSC).** Thermograms of natamycin, PLGA, unloaded and loaded lyophilized nanoparticles were recorded on a differential scanning calorimeter DSC7 (Software Pyris Series, Perkin-Elmer, The United States). Accurately weighed samples (2–10 mg) were analyzed at a scan rate of  $10^{\circ}\text{C}/\text{min}$  covering the temperature range  $25$ – $270^{\circ}\text{C}$ . Physical mixtures of PLGA and natamycin, containing similar relative proportions of polymer and preservative than the loaded nanoparticles, were blended manually in a mortar and used as a control to confirm that natamycin could be detected by DSC.

**X-ray Diffraction (XRD).** Crystalline properties of natamycin, PLGA, unloaded and loaded lyophilized nanoparticles as well as

corresponding physical mixtures PLGA–natamycin were determined by XRD. Diffraction patterns were recorded on a Brükker D8 Discover diffractometer using a Co K $\alpha$  radiation ( $\lambda = 1.788 \text{ \AA}$ ). Data were collected over an angular range comprised between  $5$  and  $50^{\circ}$  ( $2\theta$ ) with a step size of  $0.02^{\circ}$  (0.5 second per step).

### Performance Tests

**In Vitro Release Kinetics.** *In vitro* release studies were carried out using the dialysis bag technique<sup>21</sup> for the prepared nanoparticles, pure natamycin and PLGA as well as the physical mixture. Powders or lyophilized nanopowders were suspended in MilliQ water using brief ultrasonication, targeting an initial natamycin

concentration of 100 ppm. About 1 mL of these suspensions was placed in a dialysis bag (Float-A-Lyzer<sup>®</sup> G2, Biotech Grade Cellulose Ester, MWCO 8–10 kDa, Spectrumlabs, The United States) and incubated in 35 mL of MilliQ water at 25 °C in a shaking bath. Each sample was run in duplicates. Total volume was collected at predetermined intervals and replaced with equal volume of fresh release medium to maintain sink conditions. The amount of natamycin in the aliquots was assayed by the HPLC method previously described. The cumulative percentage of natamycin released was calculated for both duplicates—considering the replaced volume of release medium—and plotted versus time.

To further characterize the rate and mechanism of release of natamycin out of the nanoparticles, the release data were fitted to classical mathematical models including first-order kinetics [eq. (3)], Higuchi kinetics [eq. (4)], and Korsmeyer–Peppas model [eq. (5)].<sup>22</sup>

$$M_t/M_\infty = 1 - e^{-kt} \quad (3)$$

$$M_t/M_\infty = k \cdot t^{1/2} \quad (4)$$

$$M_t/M_\infty = k \cdot t^n \quad (5)$$

where  $M_t/M_\infty$  represents the cumulative fraction of natamycin released at the time  $t$  over the total amount released,  $k$  is the release rate constant, and  $n$  is the diffusion exponent indicative of the mechanism of natamycin release. Fittings were obtained by plotting, respectively,  $\log(100 - \%$ released) versus time (first-order) and  $\%$ released versus square root of time (Higuchi). The initial 60% of preservative released were fitted in the Korsmeyer–Peppas model by plot of  $\log(\%$ released) versus  $\log(\text{time})$  and the value of “ $n$ ” determined from the slope.<sup>23,24</sup> For swellable nanocarriers,  $n = 0.43$  represents a release mechanism based only on Fickian diffusion while  $n = 0.85$  corresponds to a case-II transport based on relaxation/swelling of the nanocarriers. Intermediate values indicate an anomalous transport and combination of both diffusion and relaxation phenomenon.

**In Vitro Antifungal Activity.** The antifungal activity of natamycin-loaded nanoparticles, physical mixtures, and pure natamycin was assessed against *Saccharomyces cerevisiae* (ATCC 9763) by agar disk diffusion assay. Briefly, a layer of nutrient OGYE agar inoculated with *Saccharomyces cerevisiae* was allowed to solidify in a Petri dish. Sterile blank disks were placed in a stainless steel cylinder and impregnated with 50  $\mu\text{L}$  of nano-suspension (nanopowders suspended in 1 mL MilliQ water with an equivalent concentration of natamycin of 100 ppm). A similar procedure was applied to standard solutions of natamycin to establish a calibration curve on the range 30–300 ppm. The disks impregnated with standards or nano-suspensions were then placed on the solidified agar layer and petri dishes were kept at 4 °C overnight to allow the diffusion of natamycin. After removal of the disks, plates were incubated at 30 °C for 24 h. The diameter of the zone of inhibition was measured and compared with a calibration curve established with the standard samples to determine the quantity of natamycin released. Disks impregnated with the nanosuspensions were transferred to a fresh Petri dish and the procedure was repeated over 5 days to follow the release of natamycin. Results are pre-

sented as cumulative activity ( $\mu\text{g}$  of natamycin released per day/total  $\mu\text{g}$  of natamycin released over 5 days) calculated from triplicate measurements.

## RESULTS AND DISCUSSION

### Formulation Development

Various methods of producing polymeric nanoparticles from preformed polymers like PLGA have been reported in the literature.<sup>25–27</sup> Due to its complex chemical structure, natamycin is incompatible with water-insoluble solvents but can be solubilized at relatively low but acceptable levels for encapsulation in polar solvents miscible with water in all proportions, such as methanol for instance.<sup>1</sup> The nanoprecipitation technique was thus considered to be the most appropriate method for the preparation of natamycin-loaded nanoparticles. Firstly described by Fessi *et al.*, this technique consists in the addition of a water-miscible organic solution (solvent phase) containing the polymer and the antifungal, into an aqueous medium (non-solvent phase).<sup>20</sup> The nanoparticles are formed instantaneously during the rapid diffusion of the solvent phase in the non-solvent phase by precipitation of the polymer. Efficient formation of nanoparticles is achievable for low concentrations of polymer and low solvent/non-solvent ratio, in the so-called “ouzo region,” out of which undesired formation of large aggregates of polymer also occurs.<sup>28</sup>

The nanoprecipitation method was pre-optimized in absence of natamycin (data not shown) by considering process parameters previously reported as critical for the formation of the nanoparticles, such as solvent nature, PLGA composition, PLGA concentration in the organic solvent, and solvent/non-solvent ratio.<sup>27,29–31</sup> The water-miscible solvent used in the nanoprecipitation process is classically selected based on the polymer involved and turns out to be acetone in most cases.<sup>27</sup> Acetone is however not suitable as such for the solubilization of natamycin and led in this specific case to the replacement of pure acetone by a binary mixture of water-miscible solvents. Methanol was chosen as second solvent allowing solubilization of natamycin up to 2.5 mg/mL. To ensure simultaneously a satisfying solubilization of both PLGA and natamycin in the organic phase and a final concentration of natamycin acceptable for antifungal applications, the ratio acetone/methanol 2:1 v/v was found the most suitable. PLGA polymers presenting various molecular weights and lactide:glycolide ratios were evaluated for nanoprecipitation using this binary mixture of solvents. It was, however, evidenced that the presence of methanol limits the compatibility of large and highly hydrophobic PLGA molecules, triggering their desolvation from the organic phase. Resomer<sup>®</sup> RG752H with a 75:25 lactide:glycolide ratio and a low molecular weight (4–15 kDa) was the preferred option for this study. It was besides decided for this research to not incorporate stabilizers or surfactants in the aqueous phase to better understand the effect of natamycin itself on the nanoparticle formation. Though stabilizers might be needed to ensure stability and reduce aggregation of the nano-suspensions overtime, it has been proven that they are not a necessary component for the obtention of nanoparticles by nanoprecipitation, in which the particle formation is mainly led by the sudden diffusion of the solvent.<sup>29,31</sup> Under



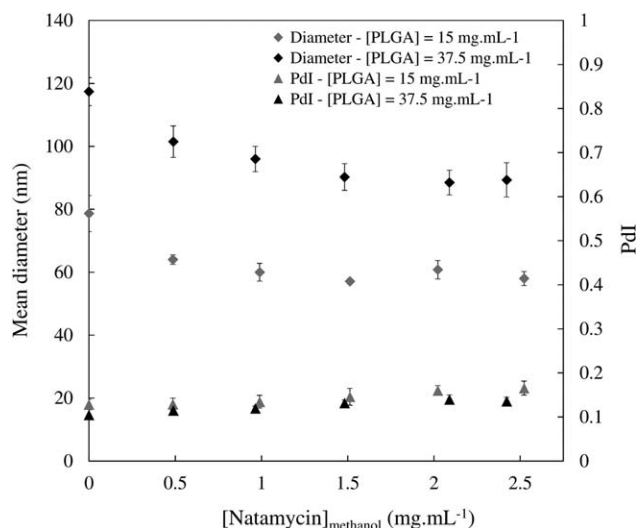


**Figure 2.** Evolution of mean diameter and polydispersity of PLGA nanoparticles as a function of natamycin concentration in methanol.

these conditions, PLGA concentration and solvent/non-solvent ratio were adjusted to obtain small nanoparticles with a controlled polydispersity and a limited formation of large aggregates. The solvent/non-solvent ratio 4% v/v and PLGA concentrations ranging from 7.5 to 37.5 mg/mL in acetone were found optimum for this purpose. Large aggregates of polymers were formed together with nanospheres for PLGA concentrations superior to 15 mg/mL.

### Physicochemical Properties

Natamycin was incorporated at 0.5–2.5 mg/mL in methanol for compositions comprising 15 and 37.5 mg/mL of PLGA in acetone. Figure 2 presents the evolution of mean particle diameters and polydispersities for the corresponding samples. Unloaded nanoparticles were found monodisperse with narrow distributions (0.1–0.15) and sizes ranging between 80 and 120 nm. Presence of large aggregates of polymer in the suspension was observed for both samples, in particular for the 37.5 mg/mL composition. Incorporation of natamycin led to an unexpected and significant decrease in mean diameters (10–30 nm) as well as to the visual disappearance of aggregates in the sample. This particle size reduction effect was observed only up to a limit concentration of natamycin (1 and 1.5 mg/mL for 15 and 37.5 mg/mL of PLGA) above which the mean diameters leveled. Polydispersity indexes slightly increased while remaining below 0.2, indicating preserved narrow distribution of the particle size. Nanometric sizes and polydispersity of natamycin-loaded nanoparticles were confirmed by TEM (Figure 3) as well as their spherical shapes and the absence of natamycin recrystallization.

Significant interactions occurring between the antifungal and the polymer in the organic phase, counteracting polymer/polymer, polymer/solvent, or polymer/non-solvent interactions, are the preferred hypothesis to explain the size variation and the disappearance of aggregates noticed while incorporating natamycin. More particularly, the behavior observed in our study matches the work performed by Beck-Broichsitter *et al.*<sup>32</sup> that showed that the incorporation of a small hydrophilic positively

charged drug salbutamol had a significant shifting effect on the ouzo region of PLGA, that is, the region where polymer concentration and S-NS ratio allow formation of nanoparticle suspensions by the nanoprecipitation technique. More specifically, the authors proved that the incorporation of salbutamol in the organic phase allowed formation of a complex polymer–drug more soluble in water than the polymer alone, resulting in the formation of nanoparticles without aggregation for higher polymer concentrations as well as in a significant reduction of size characteristics for drug-loaded particles compared with the corresponding unloaded nanoparticles. The absence of influence of natamycin incorporation on the particle size above a certain concentration is consistent with a saturation effect and maximum complexation between the antifungal and PLGA.

Zeta-potentials, encapsulation and loading efficiencies were further determined for the samples with PLGA at 37.5 mg/mL as displayed in Table I. Presence of ionized carboxyl PLGA end-groups at the surface of the nanoparticles led to negatively charged nanoparticles. Zeta-potential values were below  $-55$  mV for all compositions indicating strong repulsions between the nanoparticles and very good stability of the nanosuspensions despite the non-use of surfactant in the formulation. Slightly less negative values were observed while incorporating natamycin in the formulation and might be attributed to adsorption of natamycin molecules on the nanoparticles via electrostatic interactions between the carboxylic groups of PLGA and the amino group of natamycin. As natamycin is in a zwitterionic state in MilliQ water ( $pK_a = 4.6$ ,  $pK_b = 8.35$ ),<sup>1</sup> the resulting partial hiding of the surface charge is compensated by the presence of another carboxylic group on natamycin itself, explaining the limited variation observed.

Encapsulation efficiencies were in an intermediate range for all samples (20–36%) while loading efficiencies were relatively low and consistent with levels usually characteristic from hydrophilic

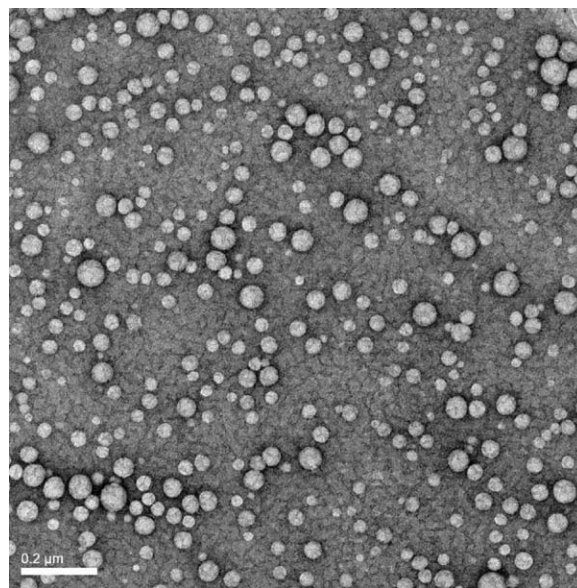


**Figure 3.** TEM micrographs of natamycin-loaded nanoparticles (formulation F6).

**Table I.** Effect of Composition on Zeta-Potential, Encapsulation, and Loading Efficiencies of Natamycin inside PLGA Nanospheres (37.5 mg/mL in Acetone)

Formulation	[Natamycin] <sub>methanol</sub> (mg/mL)	Zeta-potential ( $\zeta$ ) (mV)	EE (%)	LE (%)
F1	0	$-63.7 \pm 6.7$	—	—
F2	0.5	$-62.8 \pm 4.0$	$36.3 \pm 1.2$	$0.22 \pm 0.01$
F3	1	$-58.6 \pm 3.9$	$20.2 \pm 1.4$	$0.23 \pm 0.02$
F4	1.5	$-57.5 \pm 6.2$	$21.6 \pm 0.2$	$0.37 \pm 0.01$
F5	2	$-58.2 \pm 4.3$	$24.8 \pm 0.6$	$0.60 \pm 0.02$
F6	2.5	$-56.3 \pm 3.0$	$25.4 \pm 0.6$	$0.71 \pm 0.02$

drugs encapsulated by nanoprecipitation.<sup>31,33,34</sup> The highest encapsulation levels were observed for the lowest amount of natamycin with, similarly to mean diameters, a stabilization occurring around a concentration of 1–1.5 mg/mL in methanol, consistent with the hypothesis of a maximum complexation with PLGA molecules. Slight increase in encapsulation efficiencies for concentrations of 2–2.5 mg/mL might be explained either by additional adsorption of natamycin on the nanospheres surface without further modification of size or formation of pure natamycin crystals—both phenomena possibly decreasing artificially the level of natamycin detected in the supernatant analysis. In any case, the sustained increase of loading efficiency while incorporating higher contents of natamycin suggests its active participation to the process of nanoparticle formation and confirms what was previously observed in terms of particle size.

Loading efficiencies were found overall very limited compared with other nano-formulations reported for natamycin in the literature. Bhatta *et al.* indicated for instance a loading efficiency of up to 5.1% in chitosan/lecithins complexes,<sup>9</sup> while our group described the encapsulation of natamycin within nanoliposomes made of soybean lecithins with up to 4.4% loading.<sup>10</sup> In both cases, the preparation of nanoparticles was achieved by a preparation process similar to nanoprecipitation and it was shown that the presence of charged phospholipids or chitosan and electrostatic interactions with natamycin were the drivers of the encapsulation, similarly to what we observed here with PLGA. In both cases, however, solubilization of both natamycin and carrier materials was achievable within methanol, allowing much higher levels of incorporation of the antifungal in the initial organic phase.

Promising improvement methods for entrapment of hydrophilic drugs within PLGA nanospheres prepared by nanoprecipitation

have been evaluated at several occasions in the literature. One possible option studied by Bilati *et al.*<sup>31</sup> was for instance to promote the use of polar solvents at various levels in the solvent phase to increase the affinity of the drug for this phase and reduce leakage into the aqueous medium until the nanoparticles are formed. Though this could be an interesting option in the case of natamycin, the very limited solubility of this compound within other polar solvents than methanol and desolvation of PLGA from the organic phase while further increasing the amount of methanol involved do not offer freedom to rework the formula at this level.

Another option frequently reported in the literature to improve entrapment of hydrophilic molecules is the modification of the aqueous phase, focusing on either decreasing the solubility in water of the molecule to entrap or increasing its affinity towards the polymer. Common approaches implemented in this case are pH alteration or addition of electrolyte in the aqueous phase.<sup>33–35</sup> Further, improvements of the encapsulation of natamycin in the PLGA nano-carriers were attempted by studying the effect of pH modification (MilliQ water replaced by buffers at pH 4 and 9) or addition of NaCl (0.05–0.1% w/v). Table II summarizes diameters, PDI, encapsulation and loading efficiencies obtained for these formulations.

The pH alterations towards both acidic and alkaline pH led to 1.6–2.9 fold decreases in loading efficiencies, as well as to a significant increase in size or polydispersity of the nanoparticles. This was attributed to a change in the ionization of PLGA carboxylic groups, interfering with a proper formation of nanoparticles by the nanoprecipitation process. In the case of pH 4, a reduced presence of negatively charged carboxylic groups on PLGA, thus reduced electrostatic interactions with natamycin, is believed to be the main reason for the reduced entrapment level observed. At pH 9, the change of ionization degree of

**Table II.** Effect of Aqueous Phase Composition on Size, Encapsulation, and Loading Efficiencies of Natamycin (2.5 mg/mL in Methanol) inside PLGA Nanospheres (37.5 mg/mL in Acetone)

Formulation	Aqueous phase	Mean diameter (nm)	PdI	EE (%)	LE (%)
F6	MilliQ water	$89.3 \pm 5.4$	$0.136 \pm 0.009$	$25.4 \pm 0.6$	$0.71 \pm 0.02$
F7	Buffer pH 4	$158.3 \pm 1.6$	$0.101 \pm 0.029$	$16.4 \pm 0.6$	$0.28 \pm 0.01$
F8	Buffer pH 9	$84.2 \pm 0.4$	$0.179 \pm 0.010$	$22.2 \pm 0.8$	$0.38 \pm 0.01$
F9	NaCl 0.05% w/v	$108.4 \pm 0.3$	$0.097 \pm 0.007$	$30.7 \pm 4.0$	$0.52 \pm 0.07$
F10	NaCl 0.1% w/v	$126.6 \pm 0.7$	$0.108 \pm 0.014$	$24.9 \pm 2.2$	$0.42 \pm 0.04$

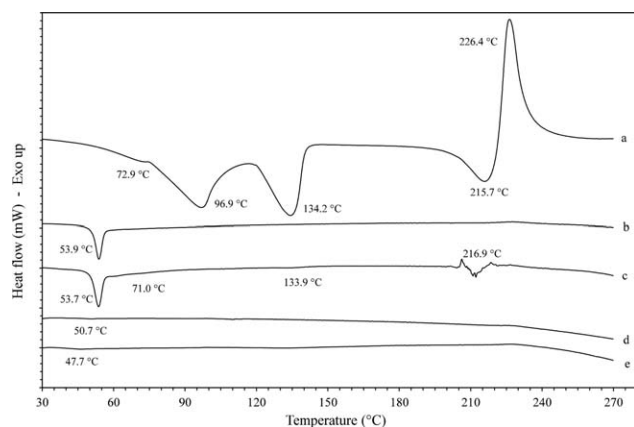


**Figure 4.** DSC thermograms of natamycin (a), PLGA (b), physical mixture PLGA/natamycin (c), unloaded (d), and natamycin-loaded PLGA nanoparticles (formulation F6) (e).

natamycin itself, transitioning from a zwitterionic to a negatively charged molecule, can also result in a lower affinity towards PLGA. It is besides known that natamycin can be solubilized at higher levels in water for extreme pHs above 4 and below 9, which can also explain the absence of benefit of pH alteration while aiming at higher encapsulation levels.<sup>1</sup>

The addition of NaCl in the aqueous phase on the other hand resulted on comparable or higher encapsulation efficiencies than in MilliQ water. The presence of electrolyte during the nanoprecipitation led however to a significant effect on the nanoparticle diameter and large quantities of aggregates visually formed. This could be attributed to the salting-out effect of NaCl or increase in viscosity created in the aqueous phase by the addition of the electrolyte, both phenomena promoting either fast precipitation of the polymer or reducing the solvent diffusion rate and consequently being unfavorable for the formation of nanoparticles.<sup>29</sup> Higher encapsulation and loading efficiencies are in this case believed to be linked to a promoted entrapment within quickly formed nanoparticles or within the large aggregates. This cannot be considered, however, as a reliable improvement method due to the low yield of nanoparticles recovered and the possible lack of homogeneity of natamycin distribution within the particles.

Using MilliQ water seems therefore to remain the optimum condition to obtain the highest levels of encapsulation in our current solvent/PLGA system.

#### Physical State of Natamycin

Information on the physical state of natamycin molecules in the nano-carriers and the possibility of interactions within the polymeric matrix of the nanoparticles were determined by differential scanning calorimetry (DSC) and X-ray diffraction (XRD).

DSC thermograms of natamycin, PLGA, loaded/unloaded nanoparticles and corresponding physical mixture PLGA–natamycin (F6) are shown in Figure 4. Natamycin was characterized by three consecutive endothermic transitions around 73, 97, and 134 °C, corresponding to the disappearance of the three molecules of water present in the trihydrate crystalline form. The

sharp endotherm and exotherm observed at 216 and 227 °C are, respectively, related to the melting and subsequent thermal decomposition of natamycin.<sup>1</sup> The pure PLGA exhibits a well-shaped endothermic event around 54 °C, corresponding to the commonly observed relaxation peak following the glass transition. Thermal degradation of PLGA starts around 230 °C, with an exothermic event at 367 °C (not displayed here). No melting point is observed as PLGA is by nature an amorphous copolymer.<sup>36</sup> The physical mixture shows the same endothermic peak related to PLGA glass transition around 54 °C. Two of the peaks related to dehydration and the exothermic event for natamycin degradation were also visible but shifted to lower temperatures, suggesting solubilization of natamycin within the polymer and/or interactions.

The endothermic event corresponding to the glass transition of PLGA remained visible for both unloaded and loaded nanoparticles but was shifted to lower temperatures with an intensified effect in presence of natamycin, corroborating the idea of complexation occurring between the PLGA and the preservative as previously evidenced by size measurements. No thermal transition related to natamycin was besides observed for loaded nanoparticles indicating that the compound might be amorphous or dispersed in a non-crystalline state in the polymeric matrix.

The physical state of natamycin was further confirmed by the analysis of XRD patterns as shown in Figure 5. Pure natamycin powder presents a crystalline pattern comparable to those previously reported for the trihydrate crystalline form.<sup>1</sup> The amorphous nature of PLGA was confirmed by the absence of diffraction pattern and presence of a broad bump. The physical mixture pattern consists in a simple superposition of both natamycin and PLGA pattern, with the presence of an amorphous zone and several diffraction peaks attributable to the preservative. XRD spectra for both nanoparticle samples were similar to PLGA alone. The complete absence of diffraction peaks corresponding to natamycin in the loaded nanoparticles—although natamycin was clearly detectable in the physical mixture—reinforces the idea that the compound may exist in an amorphous or molecularly dispersed state within the polymeric matrix.

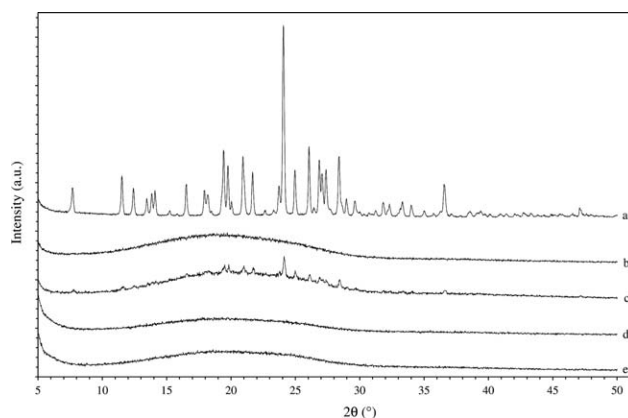


**Figure 5.** X-ray diffractograms of natamycin (a), PLGA (b), physical mixture PLGA/natamycin (c), unloaded (d), and natamycin-loaded PLGA nanoparticles (formulation F6) (e).

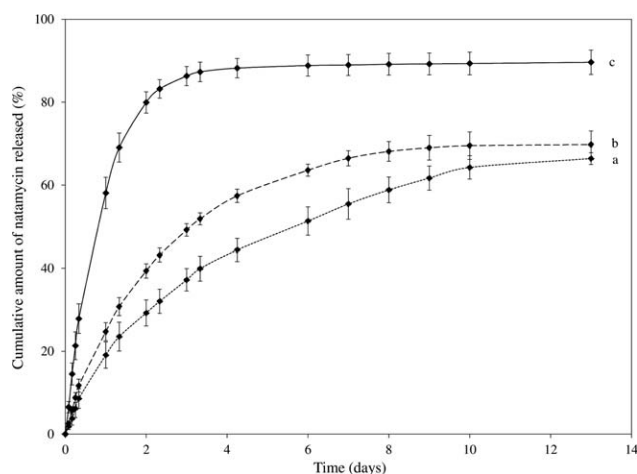


**Figure 6.** *In vitro* release profile of natamycin (a), physical mixture PLGA/natamycin (b), and natamycin-loaded PLGA nanoparticles (formulation F6) (c).

### *In Vitro* Release Kinetics

*In vitro* release kinetics profile of natamycin, physical mixture PLGA–natamycin and loaded nanoparticles (formulation F6) are displayed in Figure 6.

Pure natamycin showed a slow release pattern with continuous delivery over more than 14 days, in accordance with the progressive dissolution of its crystalline form. A noteworthy difference between pure preservative and physical mixture was observed with a clear acceleration of the release and a plateau reached after 10 days. This finding is likely to be related to the electrostatic complexation with PLGA previously mentioned, which could ease the dissolution of natamycin crystals, or possibly to PLGA hydrolysis which could have created a slightly more acidic medium in the dialysis bag, also in favor of natamycin dissolution.

Natamycin-loaded PLGA nanoparticles exhibited a faster release pattern consisting in two phases: an initial burst release of 80% over the first 2 days (29% for crystalline natamycin), followed by a continuous release at very slow rates up to 7 days. The first phase is attributable to the release of non-encapsulated natamycin, either present in solution or adsorbed at the surface of the nanoparticles, evidenced previously by limited encapsulation efficiencies and zeta-potential measurements. Higher availability of natamycin in soluble state in the case of nanoparticles is also in accordance with the amorphous state of the compound highlighted by DSC and XRD. The slow following phase is on the other hand related to the progressive release and permeation

towards the aqueous medium of natamycin encapsulated within the polymeric matrix.<sup>37</sup>

The release data were further fitted with first-order kinetics, Higuchi kinetics, and Korsmeyer–Peppas models classically applied to nano-carriers.<sup>22–24</sup> Correlation coefficients  $R^2$  and release rate constants are summarized in Table III. A molecular suspension of natamycin was analyzed as a control to determine the effect of the dialysis method itself. Release from this molecular suspension was found to obey a first-order kinetics ( $R^2 = 0.974$ ) with a very fast delivery rate (100% released reached after 2 days), in accordance with the progressive transport of molecular natamycin from the dialysis bag membrane towards the external medium induced by the sink conditions. Pure natamycin crystals presented a better fitting with the Higuchi model, which is representative from the drug dissolution and diffusion out of a crystalline matrix. Release from the physical mixture was also compatible with the Higuchi model, with as expected a release rate constant higher than in the case of natamycin alone. In the case of natamycin-loaded nanoparticles, the best fitting model and higher correlation coefficient values were found for the first-order kinetics similarly to molecular natamycin, in accordance with the presence of non-encapsulated preservative previously highlighted.

Application of the Korsmeyer–Peppas model gave very good correlations for both natamycin crystals and PLGA nanoparticles. Values of  $n$  comprised between 0.43 and 0.85 highlighted an anomalous non-Fickian diffusion mechanism for all samples. High value of  $n$  for polymeric nanoparticles indicated a large contribution of swelling/relaxation of the nanoparticles for the release of natamycin rather than a simple Fickian diffusion.

### Antifungal Performance

Figure 7 displays the cumulative antifungal activity against *Saccharomyces cerevisiae* observed over 5 days for pure natamycin, physical mixture polymer-preservative and PLGA nanoparticles loaded with various amounts of preservative (formulations F2, F4, and F6).

Natamycin presented a regular pattern with comparable levels of antifungal activity provided every day over a long period of time (>5 days), in accordance with the slow release kinetics from crystals evidenced via the dialysis bag method and then sustained release of molecular natamycin available for antifungal activity. As expected from *in vitro* release kinetics results, incorporation of PLGA in the physical mixture slightly enhanced the antifungal activity, particularly during the first day, though the

**Table III.** Correlation of Release Kinetics Data of Natamycin from Crystalline Powder, Physical Mixture, and PLGA Nanospheres (Formulation F6)

	First-order		Higuchi		Korsmeyer–Peppas	
	$R^2$	$k$ ( $10^{-2} \text{ h}^{-1}$ )	$R^2$	$k$	$R^2$	$n$
Natamycin crystals	0.940	0.48	0.988	4.23	0.975	0.708
Physical mixture PLGA–natamycin	0.902	0.71	0.974	5.32	0.983	0.763
PLGA nanospheres	0.975	3.1	0.963	10.92	0.981	0.824



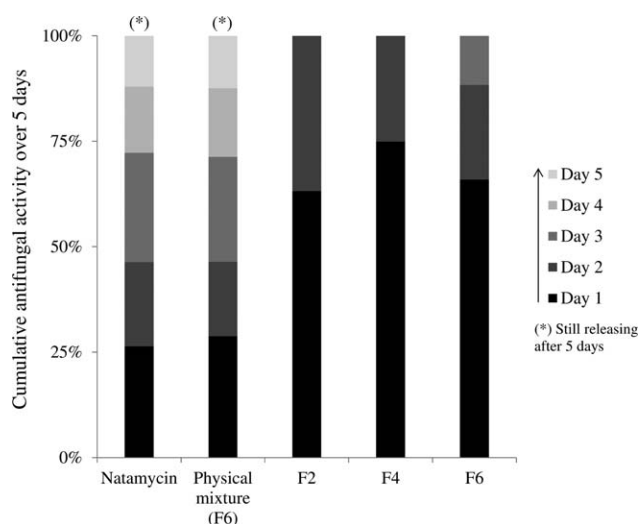


**Figure 7.** Cumulative antifungal activity observed against *Saccharomyces cerevisiae* for pure natamycin, physical mixture PLGA–natamycin and loaded nanoparticles (formulations F2, F4, and F6).

sustained pattern over 5 days remained comparable to pure natamycin.

Unloaded nanoparticles (not displayed here) did not show activity against the yeast indicating no antifungal effect of PLGA itself. Antifungal performance of natamycin-loaded nanoparticles differed clearly from the pure preservative, with the major part of the activity occurring during the first 24h at 2.4 to 3-fold higher levels compared with crystalline natamycin. Absolute cumulative release from formulations F2, F4, and F6 were, respectively, 50, 67, and 77% of the initial content of natamycin, with an absence of antifungal activity detected after 2–3 days due to quantities released too low to be detected by the disk-diffusion assay. These findings corroborate the biphasic profile established by *in vitro* release kinetics.

Compared with crystalline natamycin, the initial burst release observed for natamycin-loaded PLGA nanoparticles can be highly beneficial in terms of antifungal activity to achieve in a shorter time the minimum inhibitory concentration required towards micro-organisms. Due to the efficacy of natamycin at low doses toward most food microbes (1–3 ppm), the following slower phase can also be useful to help maintaining a sustained antimicrobial protection over a couple of days. Crystalline natamycin remains however the best option if antimicrobial protection is desired on a longer period of time.

## CONCLUSIONS

Nanoprecipitation was found to be an appropriate technique to prepare biodegradable polymeric nanoparticles loaded with natamycin. Spherical nanoparticles ranging from 60 to 120 nm were obtained with a narrow polydispersity (0.05–0.2) using low molecular weight PLGA (75:25 L:G ratio, 4–15 kDa) dissolved in a binary mixture acetone/methanol 2:1 v/v suitable for the solubilization of the antifungal and the carrier material. Incorporation of natamycin, via dissolution in the methanol phase, had limited effect on the polydispersity of the nano-

suspension but clearly participated to the nanoprecipitation process as highlighted by a diameter reduction of 10–30 nm and absence of large polymeric aggregates in the suspension. This phenomenon was attributed to the formation of a PLGA–natamycin complex more soluble in water than PLGA alone. Determination of entrapment levels and zeta-potentials indicated that the partially water-soluble nature of natamycin and preferential electrostatic interactions with the polymer led to limited entrapment of the antifungal while the remaining molecules were present in water or adsorbed at the surface of the nanoparticles. The approach of pH alteration or salt addition commonly used in the literature to maximize entrapment of charged hydrophilic drugs was not found efficient for the present solvent/PLGA/natamycin system, due to the zwitterionic nature of the antifungal molecule.

DSC and XRD analyses pointed out the presence of natamycin in an amorphous or molecularly dissolved state within the polymeric matrix. *In vitro* release profiles and antifungal activity assays confirmed that limited entrapment levels and modified physical state of natamycin promote a higher availability of free preservative molecules—at levels relevant for antimicrobial protection—and faster release rates compared with its classical crystalline form.

These findings suggest that the use of natamycin encapsulated in polymeric nanoparticles could represent an advantage for the treatment of food products for which high levels of availability and antifungal protection are required at early stages of their preparation, for instance products containing a high initial amount of moisture such as cheese. Further improvements remain nevertheless necessary to achieve superior and optimized encapsulation levels of natamycin. Possible options to explore for this purpose could include adding a stabilizer/surfactant to prevent excessive loss of preservative in the aqueous phase during the nanoprecipitation process, combining PLGA with another polymer presenting higher affinity for methanol to allow higher incorporation of natamycin initially or combining the nanoprecipitation process with purification and/or concentration steps to recover untrapped natamycin. Optimized entrapment levels of natamycin should in practice maximize antifungal protection and extend the antimicrobial benefits observed in this study, turning natamycin-loaded PLGA nanospheres into a commercially viable alternative to the current crystalline formulations.

## ACKNOWLEDGMENTS

The authors would like to acknowledge the European Union (Marie Curie Actions 7<sup>th</sup> Framework, Initial Training Network PowTech, grant agreement n°264722) and DSM Food Specialties for providing financial support to conduct this research. The authors also would like to thank Meng-Yue Wu (National Center for High Resolution Electron Microscopy (NCHREM), Delft University of Technology, The Netherlands) for helping with the TEM pictures.

## REFERENCES

1. Brik, H. In *Analytical Profiles of Drug Substances and Excipients*; Florey, K.; Bishara, R.; Brewer, G. A.; Fairbrother, J. E.; Grady, L. T.; Leemann, H.-G.; Mollica, J. A.; Rudy, B. C., Eds.; Academic Press Inc: London, **1981**; Vol.10, p 513.

2. Hamilton-Miller, J. M. T. *Bacteriol. Rev.* **1973**, *37*, 166.
3. Thomas, A. H. *The Analyst* **1976**, *101*, 321.
4. Lück, E.; Jager, M., Eds.; *Antimicrobial Food Additives: Characteristics, Uses, Effects*, 2nd ed.; Springer-Verlag: Berlin, **1997**.
5. Russell, N. J.; Gould, G. W., Eds.; *Food Preservatives*, 2nd ed.; Kluwer Academic/Plenum Publishers: New York, **2003**.
6. Te Welscher, Y. M.; Ten Napel, H. H.; Masià Balagué, M.; Souza, C. M.; Riezman, H.; De Kruijff, B.; Breukink, E. *J. Biol. Chem.* **2008**, *283*, 6393.
7. Sanguansri, P.; Augustin, M. A. *Trends Food Sci. Tech.* **2006**, *17*, 547.
8. Weiss, J.; Takhistov, P.; McClements, D. J. *J. Food Sci.* **2006**, *71*, R107.
9. Bhatta, R. S.; Chandasana, H.; Chhonker, Y. S.; Rathi, C.; Kumar, D.; Mitra, K.; Shukla, P. K. *Int. J. Pharm.* **2012**, *432*, 105.
10. Phan, C. M.; Subbaraman, L.; Liu, S.; Gu, F.; Jones, L. J. *Biomater. Sci. Polym.* **2014**, *1*, 18.
11. Bouaoud, C.; Lebouille, J. G. J. L.; Mendes, E. D.; Braal, H. E. A.; Meesters, G. M. H. *J. Liposome Res.* **2015**, *1*.
12. Kumari, A.; Yadav, S. K.; Yadav, S. C. *Colloids Surf. B* **2010**, *75*, 1.
13. Soppimath, K. S.; Aminabhavi, T. M.; Kulkarni, A. R.; Rudzinski, W. E. *J. Control. Release* **2001**, *70*, 1.
14. Abdelghany, S.; Quinn, D. J.; Ingram, R. J.; Gilmore, B. F.; Donnelly, R. F.; Taggart, C. C.; Scott, C. J. *Int. J. Nanomed.* **2012**, *7*, 4053.
15. Betancourt, T.; Brown, B.; Brannon-Peppas, L. *Nanomedicine* **2007**, *2*, 219.
16. Mohammadi, G.; Nokhodchi, A.; Barzegar-Jalali, M.; Lotfipour, F.; Adibkia, K.; Milani, M.; Azhdarzadeh, A.; Kiafar, F.; Nokhodchi, A. *Colloids Surf.* **2010**, *34*, B7.
17. Mohammadi, G.; Nokhodchi, A.; Barzegar-Jalali, M.; Lotfipour, F.; Adibkia, K.; Ehyaei, N.; Valizadeh, H. *Colloids Surf. B* **2011**, *88*, 39.
18. Van de Ven, H.; Paulussen, C.; Feijens, P. B.; Matheeußen, A.; Rombaut, P.; Kayaert, P.; Van den Mooter, G.; Weyenberg, W.; Cos, P.; Maes, L.; Ludwig, A. *J. Control. Release* **2012**, *161*, 795.
19. Zhang, L.; Pornpattananangkul, D.; Hu, C. M. J.; Huang, C. M. *Curr. Med. Chem.* **2010**, *17*, 585.
20. Fessi, H.; Puisieux, F.; Devissaguet, J. P.; Ammoury, N.; Benita, S. *Int. J. Pharm.* **1989**, *55*, R1.
21. D'Souza, S. S.; DeLuca, P. P. *Pharm. Res.* **2006**, *23*, 460.
22. Costa, P.; Sousa Loubo, J. M. *Eur. J. Pharm. Sci.* **2001**, *13*, 123.
23. Korsmeyer, R. W.; Gurny, R.; Doelker, E.; Buri, P.; Peppas, N. A. *Int. J. Pharm.* **1983**, *15*, 25.
24. Riger, P. L.; Peppas, N. A. *J. Control. Release* **1987**, *37*, 5.
25. Reis, C. P.; Neufeld, R. J.; Ribeiro, A. J.; Veiga, F. *Nanomed. Nanotechnol. Biol. Med.* **2006**, *2*, 8.
26. Vauthier, C.; Bouchemal, K. *Pharm. Res.* **2009**, *26*, 1025.
27. Rao, J. P.; Geckeler, K. E. *Prog. Polym. Sci.* **2011**, *36*, 887.
28. Stainmesse, S.; Orecchioni, A. M.; Nakache, E.; Puisieux, F.; Fessi, H. *Colloid Polym. Sci.* **1995**, *273*, 505.
29. Mora-Huertas, C. E.; Fessi, H.; Elaissari, A. *Adv. Colloid Interface Sci.* **2011**, *163*, 90.
30. Legrand, P.; Lesieur, S.; Bochot, A.; Gref, R.; Raatjes, W.; Barratt, G.; Vauthier, C. *Int. J. Pharm.* **2007**, *344*, 33.
31. Bilati, U.; Allémann, E.; Doelker, E. *Eur. J. Pharm. Sci.* **2005**, *24*, 67.
32. Beck-Broichsitter, M.; Rytting, E.; Lebhardt, T.; Wang, X.; Kissel, T. *Eur. J. Pharm. Sci.* **2010**, *41*, 244.
33. Barichello, J.; Morishita, M.; Takayama, K.; Nagai, T. *Drug. Dev. Ind. Pharm.* **1999**, *25*, 471.
34. Govender, T.; Stolnik, S.; Garnett, M. C.; Illum, L.; Davis, S. S. *J. Control. Release* **1999**, *57*, 171.
35. Peltonen, L.; Aitta, J.; Hyvönen, S.; Karjalainen, M.; Hirvonen, J. *AAPS PharmSciTech.* **2004**, *5*, 16.
36. Lendlein, A.; Sisson, A., Eds.; *Handbook of Biodegradable Polymers: Isolation, Synthesis, Characterization and Applications*; Wiley-VCH Verlag & Co: Weinheim, **2011**.
37. Fredenberg, S.; Wahlgren, M.; Reslow, M.; Axelsson, A. *Int. J. Pharm.* **2011**, *415*, 34.

**SGML and CITI Use Only**  
**DO NOT PRINT**

